A DC-AC Converter with Optimised PWM Switching Strategy for Grid-Connected PV System

Alexis de Medeiros Torres
UNIFOR/CCT/NPT
CEP: 60811-341 – Fortaleza, CE – Brazil
alexism@unifor.br

Fernando Antunes (SOBRAEP member)
UFC/DEE/GPEC
CEP: 60455-760 – Fortaleza, CE – Brazil
fantunes@dee.ufc.br

Abstract – **This work deals with the design and laboratory implementation of a power electronic converter to interconnect a PV system to the grid. The converter is made up of a dc-dc boost structure and a three-phase voltage source inverter (VSI) with optimised sinusoidal PWM strategy. The dc-dc boost converter allows the PV system to operate at maximum power point (MPPT). The VSI matches the converter voltage to the one of the grid. The optimised switching strategy used guarantees harmonics elimination at the VSI output voltage up to the 17th harmonic. The inverter uses IGBT as power switches, and is microcontroller-operated. The system was interconnected to the grid and experimental results are shown to access the performance of the system.**

I. INTRODUCTION

PV systems technologies are in fast expansion and their role in the world context have been increasing, propitiating the supply of safe energy and pollution free[1]. At the present days photovoltaic systems are still related with the supply of power to remote areas or rural electrification in developing countries, small telecommunication devices and satellites. Small and medium grid-connected PV system are been installed in several countries[2]. In these grid connected systems power electronics research has an important role in developing high efficiency converters.

This paper deals with the design and laboratory implementation of a power electronics dc-ac converter to interconnect a PV system to the grid. The dc-ac converter is part of a more complete system developed to supply the electric utility grid with photovoltaic energy. The converter is made up of a dc-dc boost structure and a three-phase voltage source inverter (VSI) with optimised sinusoidal PWM strategy. The input stage, a dc-dc boost converter allows the PV system to operate at MPPT according to information supplied through a neural network[1]. The output stage, a VSI matches the converter voltage to the one of the grid. The optimised switching strategy used guarantees harmonics elimination at the VSI output voltage up to the 17th harmonic. The converter uses IGBT as power switches, and is microcontroller-operated. Experimental results for a 700W PV system interconnected to the grid are shown to access the performance of the power electronic converter.

II. THE POWER ELECTRONICS CONVERTER

Fig.1 shows the developed system to interconnect the PV module to the grid, and in dashed lines the power electronics converter.

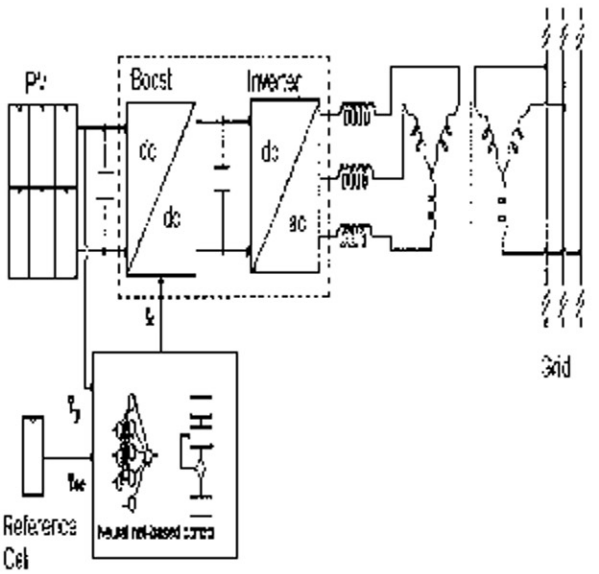

Fig. 1. The Power Electronics Converter within Dashed Lines

The PV panel is associated in such a way to provide an open circuit voltage between 129V and 137V giving an on-load input voltage range of: 91 to 105 V

The boost stage operates in the continuous conduction mode, and it makes the PV system to operate at maximum power point.

Fig.2 shows the boost stage, and it has been designed[1][3] for output voltage of 106 V, switching frequency (fc) of 33kHz and an output power of 700 W.

The converter calculated values are[4]:

Duty Cycle (D): $0 \leq D \leq 0.41$

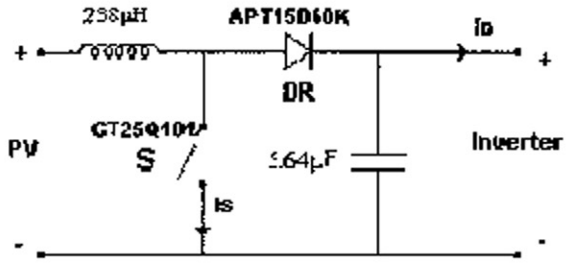

Fig. 2. Input Boost Stage

Average output current (I_o): $I_o = 7.0\ A$

Average inductor current(I_{LL}): $7{,}0A \le I_{LL} \le 8{,}15A$

Switch current (I_s),

$$I_s = \frac{I_{MIN} + 4 \bullet (I_{MIN} + I_{MAX})/2 + I_{MAX}}{6} \bullet D = 1.15A \quad (1)$$

$$I_{s(RMS)} = \sqrt{\frac{I_{MIN}^2 + 4 \bullet [(I_{MIN} + I_{MAX})/2]^2 + I_{MAX}^2}{6}} \bullet D = 3.5A \quad (2)$$

Diode current (I_D),

$$I_D = I_L - I_{GT} = 7.0\text{A} \quad (3)$$

Boost inductance(L),

$$\Delta I = \frac{V_i \bullet D}{f \bullet L} \qquad L = 238\ \mu\text{H} \quad (4)$$

Critical inductance(L_C)

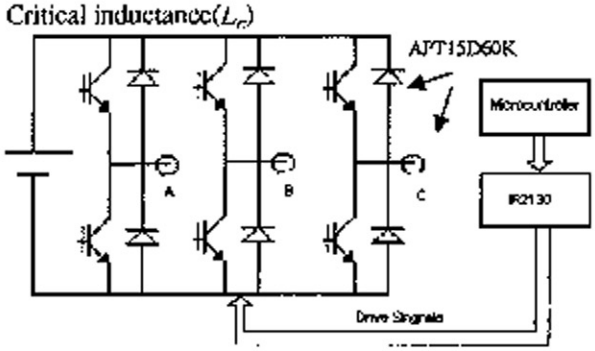

Fig. 3. Three-Phase Inverter at the Output Stage

$$L_C = \frac{0.5 \bullet R_L \bullet D \bullet (1-D)^2}{f} = 23.8\mu H \quad (5)$$

Output capacitor(C)

$$\Delta V_C = \frac{I_o \bullet D}{f \bullet C} \qquad C = 5{,}64\ \mu\text{F} \quad (6)$$

Fig.3 shows the implemented dc-ac output stage.

The two levels optimised sinusoidal PWM strategy has been chosen for the following reasons: it is necessary an inverter with six switches only (GT25Q101), while with the three levels strategy would be necessary nine switches [5], there is a three levels output voltage and the number of pulses at the output voltage is twice the number of pulses at the command level.

Using the equations below, the switching angles shown in Table I have been generated.

$$V_K = \frac{2\sqrt{3}E}{K\pi}\left[1 + 2\sum_{i=1}^{n}(-1)^i \cos KP_i\right] \quad (7)$$

Where $K = 1, 5, 7, 11, 13, 17, 19, \ldots$

TABLE I
SWITCHING ANGLES

N	0	1	2	3	4	5
	-	12°	16,24°	8,74°	10,55°	6,80°
Determined	-	-	22,06°	24,40°	16,09°	17,30°
Angle	-	-		27,76°	30,90°	21,03°
Values	-	-			32,87°	34,66°
	-	-				35,98°

Table II shows the harmonic distortion for each eliminated harmonic in the output voltage.

TABLE II
THD IN PERCENTAGE OF THE FUNDAMENTAL COMPONENT

	0	1	2	3	4	5
V5/V1	20,0	-	-	-	-	-
V7/V1	14,3	11,8	-	-	-	-
V11/V1	9,1	22,2	20,3	-	-	-
V13/V1	7,7	22,7	27,1	10,6	-	-
V17/V1	5,9	17,4	17,1	29,3	20,2	-
V19/V1	5,3	12,9	4,4	25,2	29,2	10,2
V23/V1	4,3	3,6	12,2	3,3	16,7	31,1
V25/V1	4,05	0	10,1	0,4	4,7	25,5
$V1_{rms}/V1$	0,780	0,746	0,728	0,721	0,717	0,715

The drive signals are generated by a microcontroller-based circuit in accordance to Table II. The output signals of the microcontroller serve as input signals to the IR2130 which drives the six switches of the inverter. The microcontroller used is the Intel 80X51 at a frequency of 12MHz.

III. EXPERIMENTAL RESULTS

Some experimental results are shown to demonstrate the performance of the system. Fig.4 shows the drive signal waveform to the dc-dc converter IGBT switch. The switch duty cycle changes according to the solar irradiation in order to keep the PV system at the MPP.

Fig.5 and Fig.6 show the boost inductor current and the input current to the inverter. In Fig.6 it can be seen the influence of the dc-dc switching frequency in the inverter input current.

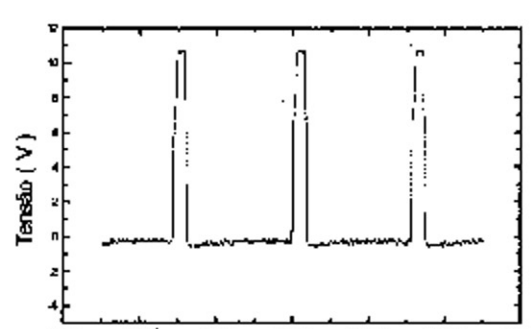

Fig. 4. DC-DC Switch drive signal

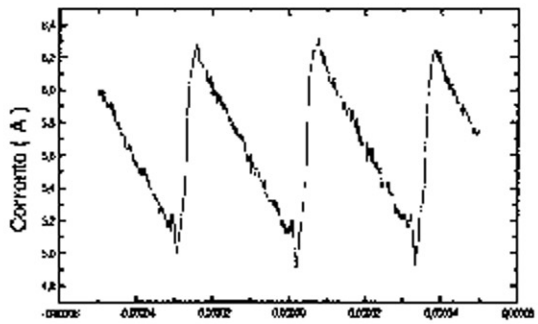

Fig. 5 boost inductor current

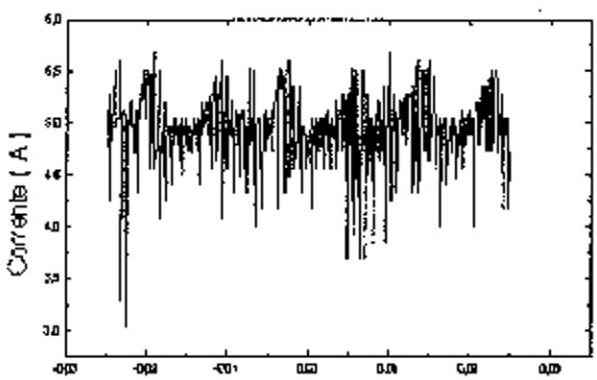

Fig. 6. Three-phase inverter input current

The following waveforms are related the VSI. Fig.7 shows the VSI input voltage. Its average value is controlled by the dc-dc converter, and is set in 106V. This value is the designed value to obtain 380V rms at the connection point to the grid(after the transformer).

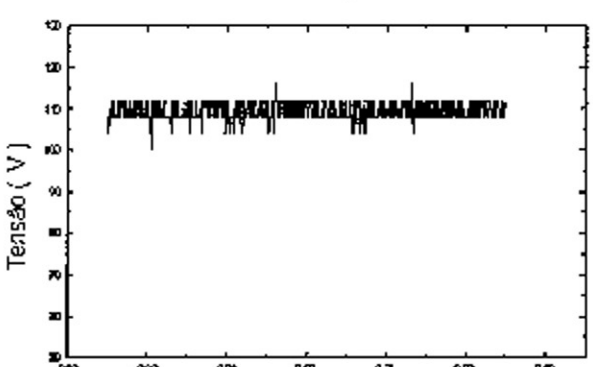

Fig. 7. Controlled Inverter Input Voltage

Fig.8 shows the voltage waveform at one of the VSI switches. It can be seen the optimised switching strategy in operation.

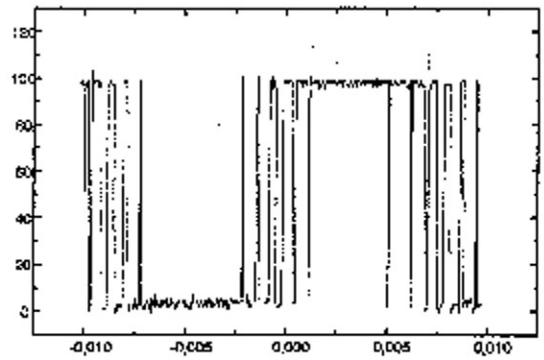

Fig. 8. Voltage across the Inverter Switches

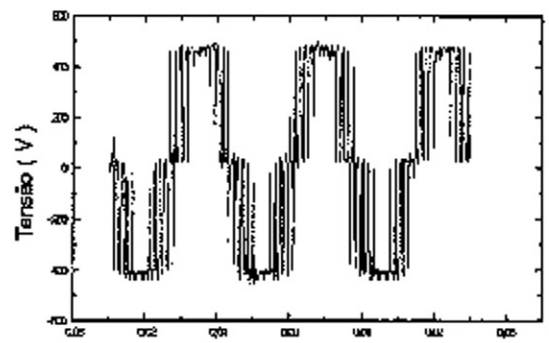

Fig. 9. inverter output voltage at the (PCC) before the connection to the Grid

Fig.9 shows the inverter output voltage at the Point of Common Connection (PCC), before the interconnection to the grid. It can be observed the switching strategy which eliminates up to the 17th harmonics at the inverter output voltage. Fig.10 shows the output voltage harmonic spectrum. The current at the PCC is seen in Fig.11, where high frequency components (above 17th harmonics) can be noted.

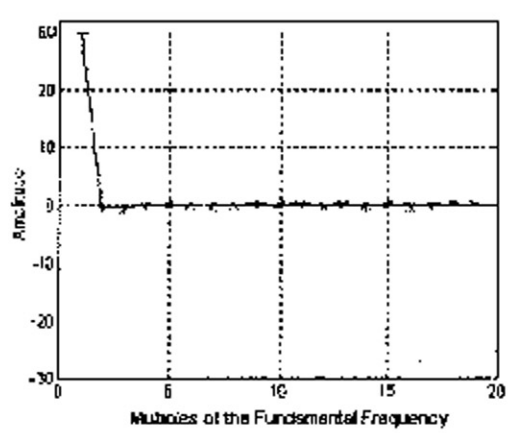

Fig. 10. Harmonic Spectrum of inverter output voltage

To show the power flow from the PV system to the grid, Fig.12 shows the voltage and current at the PCC.

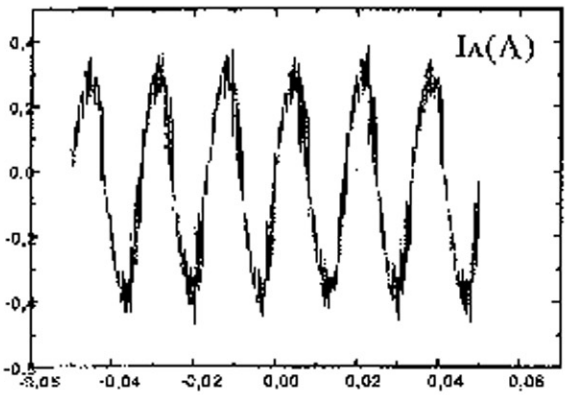

Fig. 11. Current at the PCC

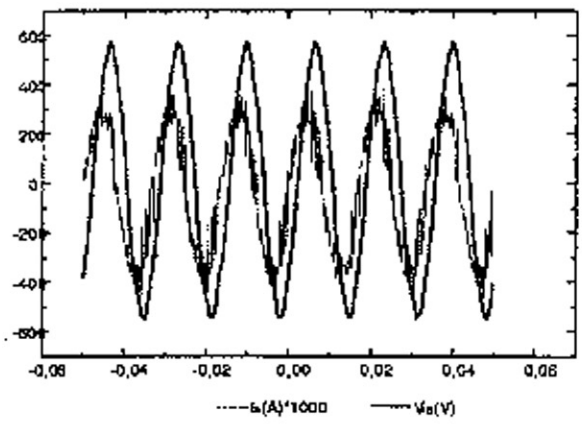

Fig. 12. Voltage and Current at the PCC

The phase difference between the voltage and current is because it has been compared line voltage to phase current. Disregarding the 30° between line and phase, voltage and current at the PCC would be near to 0° of phase, showing that the power flow is from the PV system to the grid.

IV POINT OF COMMON CONNECTION

The Fig.13 shows the PCC along with the synchronisation and protection circuits. The synchronisation circuit is provided by a voltage signal from phases B and C. At the zero crossing of the voltage of the grid an interruption is set by the synchronisation signal, and a period of the inverter output voltages is generated in phase with the voltages of the grid.

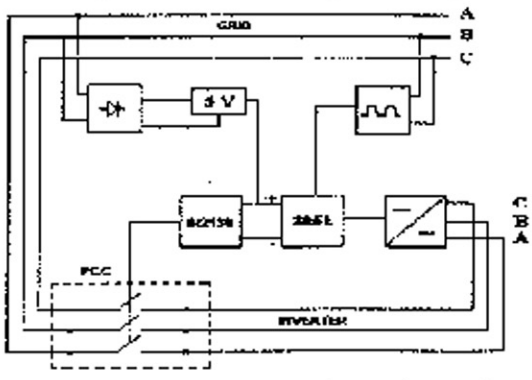

Fig. 13. Connection and protection circuit

PV systems connected to the grid may continue to operate in the event of a separation of the distribution system from the utility power source. This phenomenon is a serious threaten to safety of maintenance work. To assure the PV system is off when, for any reason, the grid is off, there is a protection circuit which acts in two ways: by disconnecting the supply voltage of the microcontroller chip and by preventing to send the drive signals to the inverter.

V. CONCLUSION

This paper has presented the design and laboratory implementation of a Power electronics converter to interconnect a PV system to the grid. The converter is made up of a dc-dc boost structure and a three-phase voltage source inverter (VSI) with optimised sinusoidal PWM strategy. The dc-dc boost converter allows the PV system to operate at MPPT according to information supplied through a neural network. The VSI matches the converter voltage to the one of the grid. The optimised switching strategy used guarantees harmonics elimination at the VSI output voltage up to the 17th harmonic.

The system has been designed for 700W and to operate at maximum power according to the solar irradiation. The MPPT is provides by the action of a neural network(discussed em[6]) in the dc-dc converter switch control strategy.

The whole system has been implemented in laboratory and the experimental results have shown the performance of the proposed system. It may be pointed out also the importance of the power electronics in the context of renewable energy.

VI. REFERENCES

[1] Torres, A. M. *Aproveitamento Fotovoltaico Controlado por Redes Neurais Artificiais Interligado ao Sistema Elétrico.* MSc Thesis, GPEC DEE UFC, Sp/98 (in Portuguese)

[2] *Manual de Engenharia para Sistemas Fotovoltaicos*, Grupo de Trabalho de Energia Solar Fotovoltaica – GTEF, Version 1.0, April, 1995.

[3] Gouveia, Daniel Xavier. *Conversor Estático Elevador para Aplicação em Sistemas Fotovoltaicos de Bombeamento d'Água.* Fortaleza:1986. 62p. Dissertação de Mestrado UFC.

[4] Mohan, N et al. *Power Electronics: Converters, Applications and Design.* John Wiley & Sons, 1st Edition.

[5] Perin, Arnaldo José. "Teoria e aplicação de modulação por largura de pulsos(PWM) com otimização de harmônicas para conversores estáticos de freqüência". *Minicurso do 6° congresso brasileiro de automática*, UFMG, Belo Horizonte, 1986, pp. 1-15.

[6] Torres, Alexis de M., Antunes, Fernando L. M., Reis, Fernando S.. "Utilization of a Neural Network Based Real Time Maximum Power Tracking Controller for Connecting a PV System to the Grid". in: *24th Annual Conference of the IEEE Industrial Eletronics Society*, , Vol 1, 1998, pp. 554-558.